A new class of highly-conducting polymer electrolyte membranes: aromatic ABA triblock copolymers

Li, Nanwen; Lee, So Young; Liu, Ying-Ling; Lee, Young Moo; Guiver, Michael D.

Publisher's version / Version de l'éditeur:
https://doi.org/10.1039/C1EE02556B
Energy & Environmental Science, 5, 1, pp. 5346-5355, 2011-11-03

Submitted to ADVANCED ENERGY MATERIALS

DOI: 10.1002/aenm.((please add manuscript number))
Full Paper

Highly Proton-Conducting Fully Aromatic Triblock Copoly(aryl ether sulfone)s

*Nanwen Li, So Young Lee, Ying-Ling Liu, Young Moo Lee *, Michael D. Guiver **

Dr. N. Li, Dr. M. D. Guiver, Prof. Y. M. Lee
WCU Department of Energy Engineering, Hanyang University, Seoul 133-791, Republic of Korea
E-mail: Michael.Guiver@nrc-cnrc.gc.ca ; ymlee@hanyang.ac.kr

S.Y. Lee, Prof. Y. M. Lee
School of Chemical Engineering, College of Engineering, Hanyang University, Seoul 133-791, Republic of Korea

Prof. Y. L. Liu
Department of Chemical Engineering, R&D Center for Membrane Technology, Chung Yuan Christian University, Taiwan

Dr. M. D. Guiver
Institute for Chemical Process and Environmental Technology, National Research Council, Ottawa, Ont, KIA OR6, Canada

Keywords: triblock copolymer; nanochannel; proton transport; fuel cell; polymer electrolyte membrane; proton exchange membrane

To achieve highly efficient proton conduction, microphase-separated morphological structure is crucial for proton exchange membranes (PEMs). Herein, we report a novel fully aromatic triblock copolymer, sulfonated poly(2,6-phenyl-1,4-phenylene oxide)-*b*-poly(arylene ether sulfone)-*b*-sulfonated poly(2,6-phenyl-1,4-phenylene oxide) (SPPO-*b*-PAES-*b*-SPPO) with highly sulfonated PPO blocks. This molecular design for a PEM was implemented to promote the nanophase separation between the hydrophobic polymer chain and hydrophilic ionic groups that are responsible for the water uptake and conduction. Morphological investigations and electrochemical measurements reveal that the proton-conducting systems derived from this triblock copolymer architecture exhibit nanoscale-organized phase separated morphology

with well-connected hydrophilic nanochannels, and thus show a dramatic enhancement in proton conductivity under partially hydrated conditions, relative to other hydrocarbon-based PEMs. The results suggest that nanoscale organization of proton-conducting functionalities is a key consideration in obtaining efficient proton transport in a partly hydrated operating environment.

1. Introduction

Proton-exchange membranes (PEMs) play a pivotal role in many technological devices, including fuel-cell vehicles, mobile devices, and stationary power units for home use.[1,2] The perfluorosulfonic acid (PFSA) class of polymers such as Nafion® (DuPont™) are most often utilized in fuel cells because of their high chemical and physical stability along with high proton conductivity, but they suffer from several problems, including high production cost, environmental incompatibility, and limited operation temperature.[3] To overcome these drawbacks, non-fluorinated hydrocarbon polymers have been investigated as alternative membranes.[3-6] Prominent among these are arylene-base PEMs because of their cost advantages, monomer safety, and structural diversity.[3] While high proton conductivities have been reported for some of these polymers, many hydrocarbon PEMs exhibit low proton conductivity in the partially hydrated state (low relative humidity); fuel cell operation under reduced humidity conditions is crucial for practical application. In the case of automotive applications, a PEM proton conductivity of close to 0.1 S/cm at 120 ^{o}C and 50 % relative humidity (RH) is the currently established guideline of the U.S. Department of Energy as target operating conditions.[3]

Proton conductivity of PEMs is closely related to several parameters such as acidity, number and position of ionic groups, main chain and/or side chain structures, composition and sequence of hydrophilic and hydrophobic components, and membrane morphology.[3,7,8]

Among these, the key parameter is believed to be membrane morphology with well-connected hydrophilic nanochannels of sulfonic acid groups, through which 'hydrated' protons can pass efficiently.[9-11] Several approaches have been examined to form hydrophilic nanochannels for arylene-based PEMs, and thus improve proton conductivity under conditions of reduced humidity and elevated temperature. These strategies have included changes in the acidity and the position of sulfonic acid groups, and the control of membrane morphologies.[6, 12-14] More recently, densely sulfonated [15-18] or sequenced hydrophilic – hydrophobic multiblock copolymers have been explored for this purpose,[19-22] but relatively little research on this class of copolymers has been done and the precise control of nanoscale morphology of multiblock copolymers may be limited due to block polydispersity.[23] Therefore, a remaining challenge in the materials science of membranes lies in the molecular design of proton-conducting nanochannels with optimized properties similar to the well-known perfluorinated polyelectrolytes.

Diblock or triblock copolymers having low polydispersity have previously been prepared using controlled/living radical polymerization techniques combined with efficient coupling reactions.[24,25] Their unique structures provide a template, where phase separation occurs on a nanometer scale due to the thermodynamic incompatibility between unlike blocks forming a variety of self-assembled morphologies including spheres arranged on a cubic lattice, hexagonally packed cylinders, interpenetrating gyroids, and alternating lamellae.[26] Various kinds of diblock or triblock copolymers with fully or partly sulfonated blocks have been studied as PEMs.[27-32] Self-organization of these block copolymers offers the opportunity for precise control of membrane morphology by manipulation of chemical compositions and relative volumes of the constituent blocks. Phase separation morphology with hydrophilic nanochannels and enhanced proton conductivity were observed for these block copolymers; however, the synthesis of most di- and tri- block copolymers relies on styrene and vinyl block

systems, in which their poor thermal and chemical stability largely limits their use in fuel cell applications.[33,34]

To avoid the instability of aliphatic chains, fully aromatic di- or tri- block copolymers could be incorporated into the molecular design, to improve the chemical and thermal stability and mechanical strength of the PEMs;[35] however, to our knowledge, they have hitherto been unreported. It is a difficult challenge to design this polymer architecture, since a mono-functional terminated aromatic block chain is required to construct the di- or tri- block copolymer. Although nucleophilic substitution polycondensation reactions generally provide stable aromatic chains for blocks, they are statistically functionalized with two different reactive groups (e.g. phenol and halogen) at each terminus. Poly(phenylene oxide) (PPO) derivatives are unique among aromatic polymers in having a mono-functional chain terminus. Different from polycondensation, PPOs are synthesized by catalyzed oxidative coupling of substituted phenols, resulting in single phenoxide-terminated chain ends.[36-38] To the best of our knowledge, PPO has never been exploited for the synthesis of fully aromatic di- or tri-block copolymers, and a systematic study on the synthesis and functionalization of such block copolymers has not yet been done. Thus, we identified mono-phenol-terminated PPO oligomers as ideal candidates for use as aromatic block chains, and our work builds upon that of researchers [39-41] who reported the synthesis of PPO derivatives with low molecular weights.

Herein, we describe the synthesis and properties of a novel class of fully aromatic triblock sulfonated poly(2,6-phenyl-1,4-phenylene oxide)-*b*-poly(arylene ether sulfone)-*b*-sulfonated poly(2,6-phenyl-1,4-phenylene oxide) (SPPO-*b*-PAES-*b*-SPPO) with highly sulfonated PPO blocks as PEMs application. The hydrophobic PAES chain is expected to be immiscible with the highly sulfonated PPO blocks, thus driving membranes to self-assemble and form nanoscale domains that contain enhanced local concentrations of sulfonic acid, which facilitate proton transport. Selected PEM properties such as thermal stability,

mechanical strength, water uptake behavior, morphological structure and proton conductivity were investigated in detail.

2. Results and Discussion

2.1. Synthesis of DiPh-PPO-F and OH-terminated PAES Oligomers

Poly(2,6-diphenyl phenylene oxide) (DiPh-PPO) oligomers with M_n of 3500 g/mol were synthesized *via* Cu(I)-catalyzed oxidative coupling reaction according to our previous report.[42] The experimental graft chain repeat units of oligomers were determined as approximately 12.3 from the ^{1}H NMR spectra, which are similar to the values determined from GPC results (Y=13.6). Subsequently, the DiPh-PPO-OH oligomers were converted to reactive fluorine-terminated oligomers (DiPh-PPO-F) by end-capping with hexafluorobenzene (HFB), since the OH-terminated PPO oligomers are reported to be capable of chain cleavage of the poly(arylene ether sulfone) (PAES) blocks under certain conditions. [15]

For the end-capping reaction with the fluorine-terminated PPO oligomers, PAES oligomers bearing –OH end groups were synthesized, as shown in **Figure 1**. The monomer composition was set so that the degree of polymerization would be 50, 70 and 100. The oligomerization reaction proceeded in NMP under typical nucleophilic substitution conditions using potassium carbonate as a catalyst. The oligomers **1** were obtained as a white fiber and characterized by viscosity measurements and GPC analyses (**Table 1**). Molecular weight distributions were in the range of 1.4 to 1.7, typical of polycondensation reactions. The experimental x values calculated from M_n were 43, 65 and 94 for x=50, 70 and 100, respectively. These values were approximately consistent with the ones expected from the comonomer feed ratios.

2.2. Synthesis and Sulfonation of Triblock Copolymers

To prepare the triblock copolymers, oligomer **1** was reacted with the activated fluorine atom of DiPh-PPO-F by nucleophilic substitution, as shown in Figure 1. The reactions proceeded smoothly, and no cross-linking and chain cleavage were evident when the temperature and reaction time were well controlled by an oil bath, which was confirmed by viscosity measurements (Table 1). The copolymers **2** were obtained as white fibers, which were soluble in chloroform, CH_2Cl_2 and NMP, but not in DMF, DMAc and DMSO. Comparison of the ^{1}H NMR spectra with those of the parent OH-terminated oligomers **1**, the polymer ^{1}H NMR spectrum showed the DiPh-PPO protons appeared at 6.28 and 7.01 ppm (**Figure 2**). These results indicate the formation of triblock copolymers.

The triblock copolymers **2** were sulfonated with chlorosulfonic acid in dichloromethane solution. Based on the number of pendent phenyl rings obtained, a five molar excess of chlorosulfonic acid was applied for the sulfonation reaction of **2**. The reaction proceeded well at room temperature, and most of the sulfonated copolymers precipitated out of solution within 15 min. The reaction was continued for an additional 15 min to ensure completion of the sulfonation reaction. However, it was important to avoid extended sulfonation time (>40 min), since insoluble gels resulted. It has been reported that strong sulfonation reagents such as chlorosulfonic acid have a tendency to cause side reactions, including crosslinking and polymer chain degradation.[43,44] In the present work, there was no evidence of chain degradation occurring under these conditions, as indicated by viscosity measurements (Table 1) and the mechanical properties of the resulting sulfonated copolymer membranes. The sulfonated products **3** were isolated as white powders, which were fully soluble only in DMSO and showed partial solubility in common polar aprotic solvents (DMF, DMAc and NMP), resulting in opaque solutions.

Figure 2 shows the ^{1}H NMR spectrum of **3**(*X*70) in the proton form. Comparison of sulfonated **3**(*X*70) with the parent non-sulfonated copolymer **2**(*X*70) reveales that the signals

assigned to the non-sulfonated pendent phenyl groups of PPO (H3, H4) disappeared, while the other aromatic protons (H5, H6, H7, H8) remained after the sulfonation reaction. A new signal assigned to the PPO sulfonated pendent phenyl groups appeared at 7.66 ppm. The absence of the H4 signal is indicative of complete sulfonation (100 % of degree of sulfonation - DS) on all the PPO pendent phenyl groups. The integration ratio of H1 to either H2 or H3 in PPO is close to 2:1, which suggests that substitution occurred only at the *para* position of the pendent phenyl groups. Moreover, these results further confirm the formation of triblock copolymers rather than the blend, since the sulfonated PPO oligomers could be dissolved readily in water. The IEC values of **3** were readily calculated by comparing the integration ratios of the isolated signals H1 and H8. As shown in Table 1, the IEC of **3** was in the range of 0.91 to 1.86 meq./g according to the ^{1}H NMR results, which were consistent with the titration values. Tough and flexible membranes were cast from DMSO solutions in the sulfonic acid form.

2.3. Morphological Structures of Triblock Copolymer 3 Membranes

The hydrophilic-hydrophobic nanophase separation morphology is particularly important for PEM materials because it affects the water uptake and the proton transport pathway in the ionomer membranes. As an example, the morphology of triblock copolymer **3**(*X*70) was investigated by tapping mode atomic force microscopy (AFM) and transmission electron microscopy (TEM). It has been shown that water adsorbed on the surface of a sample increases adhesive forces between the tip and sample.[45] This causes energy dissipation which results in a phase lag between the cantilever's oscillation and the initial oscillation imparted by the piezoelectric actuator. In our case, the ionic groups on the **3**(*X*70) membrane with an IEC value of 1.28 meq g^{-1} adsorb water, resulting in an increased phase lag. Consequently, the ionic domains of the films appear darker in the AFM phase images while the nonionic domains appear brighter. As can be seen in **Figure 3a**, the phase image exhibits a clear

hydrophilic/hydrophobic phase separation with the hydrophilic nanochannels size of 10-15 nm.

A similar behavior was also observed by investigating cross-sectional morphology of **3**(*X*70) membranes stained with lead ions. As shown in **Figure 3b**, the dark areas of TEM images correspond to the hydrophilic PPO end-capping chains while the bright domains represent the hydrophobic PAES blocks. A wormlike and interconnected hydrophilic network of small ionic clusters of 5-10 nm in size were observed, similar to the archetypical Nafion®, which has a 'cluster-network' morphology composed of ~5 to 10 nm ionic clusters interconnected by narrow ionic nanochannels.[46,47] Of considerable significance is that there is little evidence for dead end channels or larger spheroidal clusters. Moreover, small-angle X-ray scattering (SAXS) was applied to analyze the hydrophilic clusters of **3**(*X*70) triblock copolymer membrane, as shown in **Figure 4**. In general, the characteristic separation lengths between the ion-rich domains in the hydrophobic polymer-rich domains in ionomers can be observed in terms of the values of q corresponding to the so-called ionomer peak. Triblock copolymer **3**(*X*70) showed a distinct peak at 0.14 nm^{-1}, and a less distinct peak at ~0.28 nm^{-1}, suggesting longer-distance order and the lamellar microphase separation structure, as shown in Figure 4. The value of d for **3**(*X*70) membrane, calculated from $d = 2\pi/q$, was 45 nm, which is in good agreement with the TEM results, but much larger than that of Nafion.[48] This large d and unique phase-separated structure likely originate from the triblock copolymer structure, which facilitates phase separation between hydrophilic and hydrophobic aggregates to form nanochannels, and is expected to provide a nanochannel pathway for efficient proton-transport. The morphological considerations will be further discussed below with water uptake and proton conductivity properties.

2.4. Water Uptake and Dimensional Stability of 3 Membranes

Table 2 compares the density, IEC, and water uptake (weight and volume based) of **3** and Nafion membranes. As expected, higher IEC_w membranes absorbed more water due to the increased hydrophilicity. The water uptake of the **3** membranes with IEC_w values in the range of 0.97 to 1.83 meq./g was 47.4 – 91.2 % at 20 ^oC in water. However, similar values of λ (the number of H_2O molecules per sulfonic acid group) were obtained for all the membranes (Table 2). Each sulfonic acid group was solvated by approximately 26 water molecules, a value much higher than that of Nafion 112 (λ=12.0). The higher water uptake could be expected to be beneficial for proton transport.

Dimensional stability of **3** membranes was also evaluated by the water swelling ratio, which is defined as increased length or thickness of swollen membranes divided by the dimension of dry membranes. The **3** membranes showed strongly anisotropic swelling behavior, with larger dimensional change in the through-plane (thickness) direction than in the in-plane direction (**Figure 5**). This is significant in terms of fabricating a membrane electrode assembly (MEA) from a PEM, since it is important that the in-plane swelling is restricted to prevent delamination of the catalyst layer occurring from a dimensional mismatch between the two systems. For example, **3**(*X*100) membrane showed 32 % swelling ratio in the through-plane direction, in contrast to only 5 % in the in-plane direction. Other samples showed a similar tendency, which was in accordance with the behavior reported for multiblock sulfonated copolymers.[19-22] However, unlike the previously reported random or multiblock copolymers,[3] in which higher temperature induced excessive swelling, the temperature had less of an influence on the water uptake and dimensional swelling of **3** membranes, as shown in **Figure 6**. Using the **3**(*X*50) membrane (IEC_w=1.83 meq./g) as an example, the water uptake of 125 % and swelling ratio of 24 % at 100 ^oC was not excessively higher than the corresponding values at 20 ^oC (91.2 % water uptake and 16 % swelling ratio), especially when compared with other copolymer systems at this temperature difference.[3,48,49]

Although each sulfonic acid group was solvated by about 26 water molecules, at reduced relative humidity and elevated temperature, a similar but higher water uptake tendency compared with Nafion 112 was observed (**Figure 7a**). These overall results demonstrate that triblock copolymer structures, while containing a high amount of water, were effective in preventing excessive water swelling, even at elevated temperatures (> 80 ^{o}C). The morphological structure with well-connected hydrophilic nanochannels is believed to be responsible for the lower swelling ratio: the formation of small nanochannels allows for a more continuous and cohesive hydrophobic matrix that opposes the increasing osmotic pressure induced by increasing temperature.

For a more realistic comparison of the water uptake among the membranes, volumetric IEC (IEC_v, meq./cm^3) that is defined as molar concentration of sulfonic acid groups per unit volume containing absorbed water, was calculated. The IEC_v (wet) reflects the concentration of ions within the polymer matrix under hydrated conditions. The IEC_v (wet) of **3** membranes, measured at 20 °C, increased from 0.86 to 1.16 meq./cm^3, corresponding to IEC_w values increasing from 0.97 to 1.83 meq./g. All the values were lower than that of Nafion 112 under the same testing conditions (IEC_v(wet)=1.29 meq./cm^3). The increased sulfonic acid group concentration of the dry **3** membrane was retained after equilibration with water, and thus lower IEC_v (wet) values of **3** membranes in water. In contrast, the IEC_v (wet) of **3**(*X*50) membrane at reduced relative humidity is higher than that of Nafion 112 at all RHs investigated, in spite of their higher water uptake, which is the result of their relatively higher gravimetric IEC_w. As shown in **Figure 7b**, the IEC_v values became lower with increasing humidity due to increased water volume within the polymer matrix. Nafion 112 and **3**(*X*70) membrane showed approximately the same IEC_v values throughout the measured range of relative humidity, since the differences in their gravimetric IEC were counterbalanced by the differences in their density of 1.98 g/cm^3 for Nafion and 1.39 g/cm^3 for **3**(*X*70).

2.5. Proton Conductivities of 3 Membranes.

Proton conductivity for **3** membranes in liquid water at 20 ^{o}C was determined and the values are listed in Table 2. Compared to Nafion membranes, all of **3** membranes displayed higher proton conductivities. With increasing IEC_w values from 0.97 to 1.83 meq./g, proton conductivities of **3** membranes increased from 0.13 to 0.19 S/cm at 20 ^{o}C in water. These values are much higher than the Nafion 112 membrane (0.09 S/cm, at 20 ^{o}C). To further elucidate the proton-conducting properties of the triblock copolymer membranes, the proton diffusion coefficients (D_σ) through the membranes were estimated from the proton conductivity and the IEC_v(wet). As shown in Table 2, the proton diffusion coefficients (D_σ) through the triblock **3** membranes are two times higher than that of Nafion 112, in spite of their lower IEC_v(wet) values. It is assumed that the triblock polymer structure and highly sulfonated pendent sulfonic acid groups influence the size and shape of the hydrophilic ionic domains through which proton transport occurs. The morphological transition occurring over the triblock-shaped regime decreased the morphological barrier, thereby resulting in the formation of effective nanochannels for proton transport, as observed by AFM and TEM above, which results in the high D_σ values, and thus higher proton conductivities of **3** membranes. The proton conductivity over the 20-100 ^{o}C range in water was studied and the conductivity values are reported in **Figure 8**. The **3** membranes show qualitatively Arrhenius-type increases in conductivity with temperature. Higher temperatures increase the conductivity due to the enhanced charge transport. The experimental evidence revealed that the proton conductivity displays a remarkably stable behaviour, with values above 2×10^{-1} S cm^{-1} even at 100 ^{o}C-the temperature at which water evaporation dramatically affects the hydration of Nafion membrane.

Furthermore, the humidity dependence of proton conductivity was measured for **3** and Nafion 112 membranes at 90 ^{o}C. Surprisingly, we observed high conductivity values (~10^{-2}

to > 10^{-1}S cm^{-1}) for **3** membranes over a large range of 30-90 % relative humidity (**Figure 9a**); values were higher or similar in comparison to that of Nafion, even at the lowest IEC values. **3**(*X*100) with the IEC value of only 0.97 meq.g^{-1} displayed a proton-conductivity value of 0.9×10^{-2} S cm^{-1} at 30 % relative humidity. If the density of **3**(*X*100) (1.39 g/cm^3) and Nafion (1.98 g/cm^3) are taken into account, the volumetric IEC value of 1.35 meq./cm^3 for **3**(*X*100) is much lower than that of Nafion (1.78 meq./cm^3). Thus, the well-connected hydrophilic proton conducting nanochannel morphology in the triblock copolymers contributes strongly to the high proton conductivity. To further explore the reliability of the triblock copolymers, we monitored the proton-conductivity values at 30 % relative humidity over a period of 24 hours. **Figure 9b** clearly shows that the proton conductivity is nearly constant over the monitoring period. These results corroborate the robustness and reliability of fully aromatic triblock copolymers comprising highly sulfonated blocks.

Figure 10 compares the proton diffusion coefficients (D_σ) as a function of IEC_v at reduced relative humidity.The Nafion region for D_σ is from 2.67×10^{-6} to 2.62×10^{-5} cm^2/s, which is slightly narrower than that of the triblock copolymer membranes. The wider range of D_σ for the triblock-shaped **3** membranes implies that they are more dependent on relative humidity, in common with most aromatic ionomers, though to a much lesser extent. At 90% RH, which corresponds to the uppermost data point for each membrane sample, the D_σ values were higher than that of Nafion 112. Therefore, the **3** membranes have higher proton conductivity than Nafion at high RH values. Even the **3**(*X*100) membrane showed a higher D_σ value at 90% RH, in spite of having a similar IEC_v(dry) to Nafion. In addition, the triblock **3** membranes still displayed relatively good D_σ values of about 2.0×10^{-6} cm^2/s even at 30% RH, which was comparable to that of Nafion 112 (2.67×10^{-6} cm^2/s) and much higher than those of previously reported segmented or multiblock copolymer membranes.[50] The results are congruent with the above-mentioned morphological data and validate our strategy of fully

aromatic triblock copolymers with highly sulfonated blocks having pendent sulfonic acid groups for highly proton conductive ionomer membranes.

2.6. Mechanical and Thermal Properties of 3 membranes.

As shown in **Figure 11**, the mechanical property stress *vs* strain curves were affected by the length of poly(arylene ether sulfone) block because of the differences in molecular weight. The **3** membranes in the dry state at ambient conditions had tensile stress in the range of 19.7-34.4 MPa and elongation at break values of 18.7-46.2 %, with the higher IEC values having lower tensile stress. Although the mechanical properties did not match those of some of our previously reported ionomers,[49,50] the properties are adequate, and reasonable when taking into account the higher water uptake of the triblock membranes. We attribute this to the hydrophilic water-containing domains formed by the proton-conducting blocks that segregate the hydrophobic main chain, resulting in weaker physical interactions between hydrophobic blocks and lower mechanical strength of the membranes. In addition, the triblock membranes did not show any peaks after initial elongation, which is often observed in the random or other block copolymer membranes.[49] Since this behavior is regarded as the onset of disentanglement of bundles in the hydrophobic components, the results support the idea that the hydrophobic interaction is less strong in the triblock copolymer membranes.

The TGA curves of **3** membranes are shown in **Figure 12**. A two-step degradation profile as observed for all membranes in their acid form. There was no weight loss up to 200 ^{o}C because all the samples were preheated at 150 ^{o}C for 20 min to remove absorbed water. The first weight loss occurred above 250 ^{o}C, which is associated with the degradation of the sulfonic acid groups. This value is much higher than that of di- or tri-block copolymers containing polystyrene sulfonic acid,[12] indicating that the sulfonic acid groups attached to the fully aromatic polymer chain have higher thermal stability.The main weight loss at around

500-600 ^{o}C is related to the degradation of the polymer chain. The glass-transition temperature (T_g) data for triblock **3** membranes were above 200 ^{o}C, as listed in Table 2, but lower than the decomposition temperature (about 250 ^{o}C). Their high thermal stabilities presents the possibility of preparing membrane electrode assemblies (MEA) by hot pressing.

3. Conclusion

A novel class of fully aromatic triblock copolymers was synthesized for the first time by exploiting mono-phenoxide-terminated poly(phenylene oxide) oligomer end-capped onto poly(arylene ether sulfone). The resulting copolymers were subsequently post-sulfonated to get triblock sulfonated copolymers containing highly sulfonated blocks, and the degree of sulfonation of phenylated PPO side-chains was almost 100 %. Although one of the copolymer membranes **3**(*X*100) had a low IEC value (IEC=0.97 meq./g), it maintained good proton conductivity comparable to Nafion 112, even at low relative humidity (30% RH). The membranes exhibited strongly anisotropic dimensional swelling, with very low dimensional change in-plane. It appears that the unique polymer architecture brought about by nanophase separation between the extreme opposing hydrophobic and hydrophilic domains is responsible for the high proton diffusion coefficients, and thus high proton conductivities, throughout a wide range of relative humidity conditions. The results suggest that careful consideration of polymer architecture and nanoscale morphology is a key element in the design of efficient PEMs. The combination of high thermal stability, good mechanical properties and excellent proton conductivity makes triblock copolymer membranes attractive as PEM materials for further study in fuel cell applications.

Additionally, the PPO end-capped platform is versatile because it can be prepared to contain either methyl or aryl groups, which may be further modified for various applications. For example, PPO methyl groups can be modified by bromination, followed by quaternary

ammonium or ATRP for water treatment applications or anion exchange membranes. Thus, fully aromatic triblock copolymer architecture based on PPO oligomers provides new and more stable structures with interesting properties that have the potential to address various industrial and energy applications. Further investigations on this class of copolymers are ongoing in our laboratory.

4. Experimental Section

Materials: Bis(4-fluorophenyl) sulfone (DFDPS) was obtained from Sigma-Aldrich and dried under vacuum at room temperature overnight. 4,4'-(Hexafluoroisopropylidene)diphenol (6F-BPA) was purchased from Sigma-Aldrich and recrystallized twice from toluene. Hexafluorobenzene (HFB) end-capped poly(2,6-phenyl-1,4-phenylene oxide) oligomer (PPO-F) was prepared according to our previous report. [42]

*Synthesis of poly(arylene ether sulfone) (PAES) oligomers **1***: A typical synthetic procedure for OH-terminated polymer, illustrated by the preparation of **1**(*X*50) copolymers, is described as follows. Into a three-neck flask equipped with a mechanical stirrer, Dean-Stark trap, and an argon gas inletwere added 20 mmol of DFDPS, 24 mmol of 6F-BPA, and 30 mmol of K_2CO_3. Then, 30 mL of NMP and 15 mL of toluene were charged into the reaction flask under an argon atmosphere and the reaction mixture was heated to 145 °C. After dehydration and removal of toluene for several hours, the reaction temperature was increased to about 170 °C. When the increase of the solution viscosity became obvious, the mixture was cooled to room temperature and coagulated into a large excess of deionized water with vigorous stirring. The resulting fibrous copolymer was washed thoroughly with water or ethanol several times and dried under vacuum at 100 °C for 24 h. The copolymer was denoted **1**(*X*50), where (*X*50) refers to the expected length of PAES chain. Yield: 95%.

Synthesis of the triblock copolymers ***2****:* The described copolymers are denoted as **2**(*Xx*, where *x* refers to the expected length of polymer chain). **1**(*X100*) (2.0 g, 0.07 mmol of OH group), DiPh-PPO-F (0.37 g, 0.10 mmol), K_2CO_3 (0.01 g, 0.07 mmol), 15 mL of NMP, and 5 mL of toluene were added into an argon flushed reactor equipped with a Dean-Stark trap. The reaction mixture was heated to 105 ^oC for 12 h and then the reaction temperature was gradually increased over a period of 6 h to ~160 ^oC, then maintained at this temperature for an additional 20 h. The mixture was coagulated into a large excessof dilute HCl (5 wt %) with vigorous stirring and the polymer washed with water. The resulting triblock copolymers **2**(*X*100) were dried under vacuum at 100 ^oC for 24 h.

Sulfonation of the triblock copolymer: To a round-bottomed flask containing 1.0 g of **2**(*X*50) was added dry dichloromethane (40 mL) from a dropping funnel. To the mixture was added dropwise a solution of chlorosulfonic acid (0.6 mL, 3 mmol) in dry dichloromethane (20 mL) at room temperature, and the mixture was stirred vigorously at this temperature for 30 min until a brown product precipitated out of the solution..The precipitate was filtered, and washed with water several times and dried overnight under vacuum at 80 °C for 10 h to give sulfonated triblock copolymers **3**(*X*50).

Preparation of membranes: A solution of the obtained sulfonated copolymer (1 g) in DMSO (10 mL) was filtered (10 μm filter) and then cast onto a flat glass plate with a doctor blade. The cast solution was dried at 80 ^oC overnight to give a transparent, tough film. The film was dried further in a vacuum oven at 100 ^oC for 20 h. The resulting film was treated with 2 M H_2SO_4 for 24 h, washed with water several times, and dried at room temperature.

Measurements: ^1H NMR spectra were measured at 300 MHz on an AV 300 spectrometer using DMSO-d_6 or $CDCl_3$ as solvent. Ion exchange capacities (IEC) of the membranes were determined by back-titration and ^1H NMR results. A piece of the membrane was equilibrated

in a large excess of 0.5 M NaCl aqueous solution for 3 days. The released HCl by the ion exchange was titrated with standard 0.01 M NaOH solution. The reduced viscosities were determined on 0.5 g dL^{-1} concentration of polymer in NMP or DMSO with an Ubbelohde capillary viscometer at 30 ± 0.1 °C. Tensile measurements were performed with a mechanical tester Instron-1211 instrument at a speed of 1 mm/min. The thermogravimetric analyses (TGA) were obtained in nitrogen with a Perkin-Elmer TGA-2 thermogravimetric analyzer at a heating rate of 10 °C/min. The glass-transition temperature (T_g) was determined on a Seiko 220 DSC instrument at a heating rate of 20 °C/min under nitrogen protection. T_g is reported as the temperature at the middleof the thermal transition from the second heating scan.The molecular weights of polymers were determined by gel permeation chromatography (GPC) using a Waters 515 HPLC pump, coupled with a Waters 410 differential refractometer detector and a Waters 996 photodiode array detector. THF was used as the eluant and the μ-Styragel columns were calibrated by polystyrene standards.

Membrane densities were determined from membrane dimensions and weights after drying at 100 °C for 8 h. Water uptake was measured after drying the membrane in acid form at 100 °C under vacuum overnight. The dried membrane was immersed in water and periodically weighed on an analytical balance until a constant weight was obtained, giving the weight-based (IEC_w) water uptake. The volume-based IEC (IEC_v) was obtained by multiplying the membrane density by the IEC_wvalues, which were estimated from the copolymer structure. This calculation resulted in IEC_v (dry) based on the dry membrane density. The IEC_v (wet) (meq./cm^3) was then calculated based on membrane water uptake, using the following **Equation 1**.

$$IEC_v(wet) = \frac{IEC_w}{\frac{1}{\rho_{polymer}} + \frac{WU(wt\%)}{100 \times \rho_{water}}} \qquad (1)$$

where IEC_w is the gravimetric IEC (meq./g) and ρ (g/cm^3) is the density.

Proton conductivity (σ, Scm^{-1}) of each membrane coupon (size: 1 cm×4 cm) was obtained using $\sigma=d/L_sW_sR$ (d is the distance between reference electrodes, and Ls and Ws are the thickness and width of the membrane, respectively). The resistance value (R) was measured over the frequency range from 100 mHz to 100 kHz by four-point probe alternating current (ac) impedance spectroscopy using an electrode system connected with an impedance/gain-phase analyzer (Solartron 1260) and an electrochemical interface (Solartron 1287, Farnborough Hampshire, ONR, UK). The membranes were sandwiched between two pairs of gold-plate electrodes. The conductivity measurements under fully hydrated conditions in the longitudinal direction were carried out with the cell immersed in liquid water. Proton conductivity under partially hydrated conditions was performed at 90 ^oC. Membranes were equilibrated at different relative humidity for 2 h in a humidity-temperature oven before each measurement.

From the conductivity and density data, proton diffusion coefficients (D_σ) were calculated using the Nernst-Einstein **Equation 2**

$$D_\sigma = \frac{RT}{F^2}\frac{\sigma}{c(H^+)} \qquad (2)$$

where R is the gas constant, T is the absolute temperature (K), F is the Faraday constant, and $c(H^+)$ is the concentration of proton charge carrier (mol/L).

Transmission electron microscopy (TEM) observations, the membranes were stained with lead ions by ion exchange of the sulfonic acid groups in 0.5 M lead acetate aqueous solution, rinsed with deionized water, and dried in vacuum oven for 12 h. The stained membranes were embedded in epoxy resin, sectioned to 90 nm thickness with Leica microtome Ultracut UCT, and placed on copper grids. Electron micrographs were taken with a Hitachi H7600 transmission electron microscope using an accelerating voltage of 80 k.

Small angle X-ray scattering (SAXS, MXP3, Mac Science) was measured for **3** membranes at 50 % RH and room temperature. The membranes were enveloped in a Mylar bag and irradiated by X-ray (CuK_α, λ_i =1.54 Å) with 40 kV. The range of scattering vectors explored ($q = 4\pi\sin 2\theta/\lambda_i$) was from 0.085 to 3.0 nm^{-1}, where λ_i and 2θ are the incident wavelength and total scattering angle, respectively.

Acknowledgements

This research was supported by the WCU (World Class University) program, National Research Foundation (NRF) of the Korean Ministry of Science and Technology (No.R31-2008-000-10092-0), which we gratefully acknowledge.

Received: ((will be filled in by the editorial staff))
Revised: ((will be filled in by the editorial staff))
Published online: ((will be filled in by the editorial staff))

[1] M. Z. Jacobson, W. G. Colella, D. M. Golden, *Science* **2005**, *308,* 1901-1905.

[2] B. C. H. Steele, A. Heinzel, *Nature* **2001**, *414,* 345-352.

[3] M. A. Hickner, H. Ghassemi, Y. S. Kim, B. R.Einsla, J. E. McGrath, *Chem. Rev.* **2004,** *104,* 4587–4612.

[4] M. Rikukawa, K. Sanui, Prog. Polym. Sci. **2000,** *25,* 1463–1502.

[5] M. A. Hickner, B. S. Pivovar, *Fuel Cells* **2005**, *5*, 213–229.

[6] T. Higashihara, K. Matsumoto, M. Ueda, *Polymer* **2009**, *50*, 5341–5357.

[7] H. Ghassemi, J. E. McGrath, T. A. Zawodzinski, *Polymer* **2006,** *47,* 4132–4139.

[8] B. Bae, K. Miyatake, M. Watanabe, *Macromolecules* **2009**, *42,* 1873–1880.

[9] O. Diat, G. Gebel, *Nature Mater.* **2008,** *7,* 13–14;

[10] K. Schmidt-Rohr, Q. Chen, *Nature Mater.* **2008,** *7,* 75–83;

[11] J. A. Elliott, S. Hanna, A. M. S. Elliott, G. E. Cooley, *Macromolecules* **2000,** *33,* 8708–8713.

[12] E. M. W. Tsang, Z. Zhang, Z. Shi, T. Soboleva, S. Holdcroft, *J. Am. Chem. Soc.* **2007**, *129*, 15106 – 15107.

[13] H. Ghassemi, J. E. McGrath, T. A. Zawodzinski, *Polymer* **2006,** *47,* 4132 – 4139

[14] T. J. Peckham, S. Holdcroft, *Adv. Mater.* **2010,** *22,* 4667-4690.

[15] S. Matsumura, A. R. Hlil, C. Lepiller, J. Gaudet, D. Guay, Z. Shi, S. Holdcroft, A. S. Hay, *Macromolecules* **2008,** *41,* 281 – 284.

[16] S. Tian, Y. Meng, A. S. Hay, *Macromolecules* **2009,** *42,* 1153 – 1160.

[17] K. Matsumoto, T. Higashihara, M. Ueda, *Macromolecules* **2009**, *42*, 1161-1166.

[18] C. C. de Araujo, K. D. Kreuer, M. Schuster, G. Portale, H. Mendil-Jakani, G. Gebel, J. Maier, *Phys. Chem. Chem. Phys.* **2009,** *11,* 3305 – 3312.

[19] B. Bae, T. Yoda, K. Miyatake, H. Uchida, M. Watanabe, *Angew. Chem., Int. Ed.* **2010,** *49,* 317–320.

[20] A. S. Badami, A. Roy, H.-S. Lee, Y. Li, J. E. McGrath, *J. Membr. Sci.* **2009,** *328,* 156 – 164.

[21] H. S. Lee, A. Roy, O. Lane, S. Dunn, J. E. McGrath, *Polymer* **2008,** *49,* 715 – 723

[22] K. Nakabayashi, T. Higashihara, M. Ueda, *J. Polym. Sci.: Part A: Polym. Chem.* **2010,** *48,* 2757–2764.

[23] Y. Yang, S. Holdcroft, *Fuel Cells* **2005**, *5*, 171-186.

[24] C. J. Hawker, *J. Am. Chem. Soc.* **1994,** *116*, 11185–11186.

[25] V. Percec, T. Guliashvili, J. S. Ladislaw, A. Wistrand, A. Stjerndahl, M. J. Sienkowska, M. J. Monteiro, S. Sahoo, *J. Am. Chem. Soc.* **2006**, *128*, 14156–14165.

[26] I. W. Hamley, *The Physics of Block Copolymers*; Oxford University Press: New York, **1998**.

[27] T. A. Kim, W. H. Jo, *Chem. Mater.* **2010**, *22,* 3646–3652.

[28] K. Xu, K. Li, P. Khanchaitit, Q. Wang, *Chem. Mater.*, **2007,** *19*, 5937–5945.

[29] J. Gao, Y. Yang, D. Lee, S. Holdcroft, B. J. Frisken, *Macromolecules* **2006,** *39,* 8060-8066.

[30] Y. Yang, Z. Shi, S. Holdcroft, *Macromolecules* **2004**, *37*, 1678.

[31] M. J. Park, K. H. Downing, A. Jackson, E. D. Gomez, A. M. Minor, D. Cookson, A. Z. Weber, N. P. Balsara, *Nano Lett.*, **2007,** 7, 3547–3552.

[32] T. Saito, H. D. Moore, M. A. Hickner, *Macromolecules* **2010,** *43*, 599–601

[33] R. Borup, J. Meyers, B. Pivovar, Y.S. Kim, R. Mukundan, N. Garland, D. Myers, M. Wilson, F. Garzon, D. Wood, P. Zelenay, K. More, K. Stroh, T. Zawodzinski, J. Boncella, J.E. McGrath, M. Inaba, K. Miyatake, M. Hori, K. Ota, Z. Ogumi, S. Miyata, A. Nishikata, Z. Siroma, Y. Uchimoto, K. Yasuda, K.I. Kimijima, N. Iwashita, *Chem. Rev.* **2007,** *107,* 3904–3951.

[34] D. S. Kim, Y. S. Kim, M. D. Guiver, J. Ding, B. S. Pivovar, *J. Power Sources*, **2008**, *182,* 100-105.

[35] J. E. Harris, R. N. Johnson, *Encyclopedia of Polymer Science and Engineering* (Eds.: H. F. Mark, N. M. Bikales, C. G. Overberger, G. Menges), Wiley, New York, **1988,** pp. 196 – 211.

[36] A. S. Hay, *J. Polym. Sci., Part A: Polym. Chem.* **1998**, *36,* 505–517;

[37] T. Xu, D. Wu, L. Wu, *Prog. Polym. Sci.* **2008,** *33,* 894–915;

[38] K. P. Chan, D. S. Argyropoulos, D. M. White, G. W. Yeagers, A. S. Hay, *Macromolecules* **1994,** *27,* 6371-6375.

[39] S. Hay, *Macromolecules* **1969,** *2,* 107-108.

[40] K. Mühlbach, V. Percec, *J. Polym. Sci., Part A: Polym. Chem.* **1987,** *25,* 2605-2627.

[41] K. Saito, T. Tago, T. Masuyama, H. Nishide, *Angew. Chem. Int. Ed.* **2004,** *43,* 730 –733.

[42] N. Li, C. Wang, S. Y. Lee, C. H. Park, Y.M. Lee, M. D. Guiver, *Angew. Chem. Int. Ed. submitted.*

[43] A. Linkous, H. R. Anderson, R. W. Kopitzke, G. L. Nelson, *Int. J. Hydrogen Energy* **1998,** *23*, 525–529.

[44] L. Jia, X. Xu, I. Zhang, J. Xu, *J. Appl. Polym. Sci.* **1996,** *60,* 1231–1237.

[45] P. J. James, M. Antognozzi, J. Tamayo, T. J. McMaster, J. M. Newton, M. J. Miles, *Langmuir* **2001**, *17,* 349.

[46] W. Y. Hsu, T. D. Gierke, *Macromolecules* **1982**, *15*, 101-105.

[47] L. Rubatat, A. L. Rollet, G. Gebel, O. Diat, *Macromolecules* **2002**, *35*, 4050-4055.

[48] G. Gebel, *Polymer* **2000**, *41*, 5829-5838

[49] Li, N.; Shin, D.W.; Hwang, D. S.; Lee, Y. M.; Guiver, M. D. *Macromolecules* **2010,** *43*, 9810-9820.

[50] Bae, B.; Miyatake, K.; Watanabe, M. *Macromolecules* **2010**, *43*, 2684–2691.

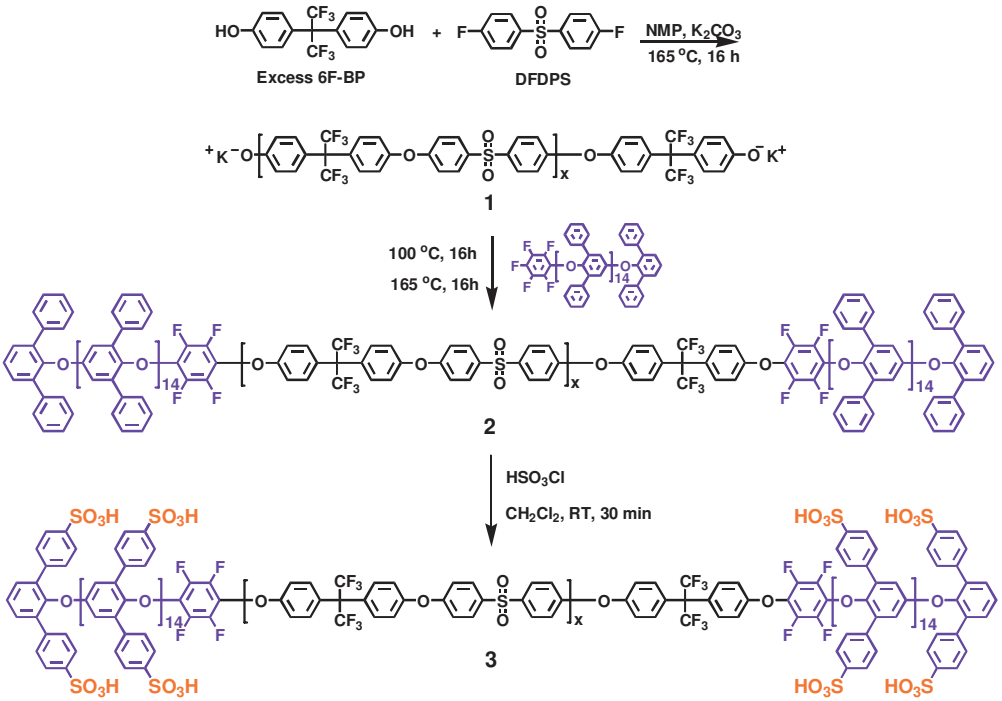

Figure 1. Synthesis of triblock copolymers **3**.

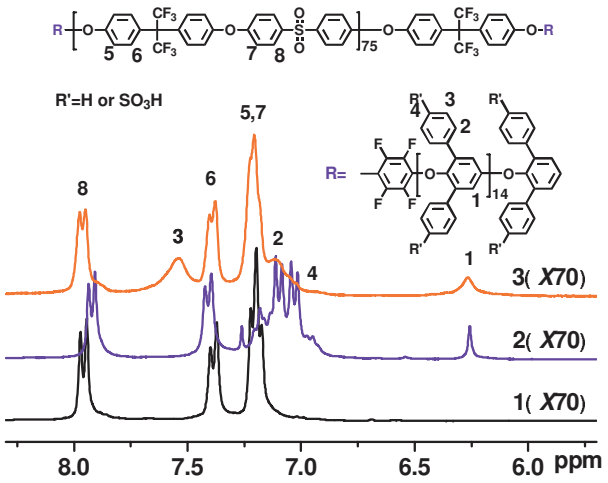

Figure 2. The ^{1}H NMR results of **1**(*X*70) in DMSO-d_6, non-sulfonated triblock copolymers **2**(*X*70) in $CDCl_3$, and sulfonated triblock copolymers **3**(*X*70) in DMSO-d_6.

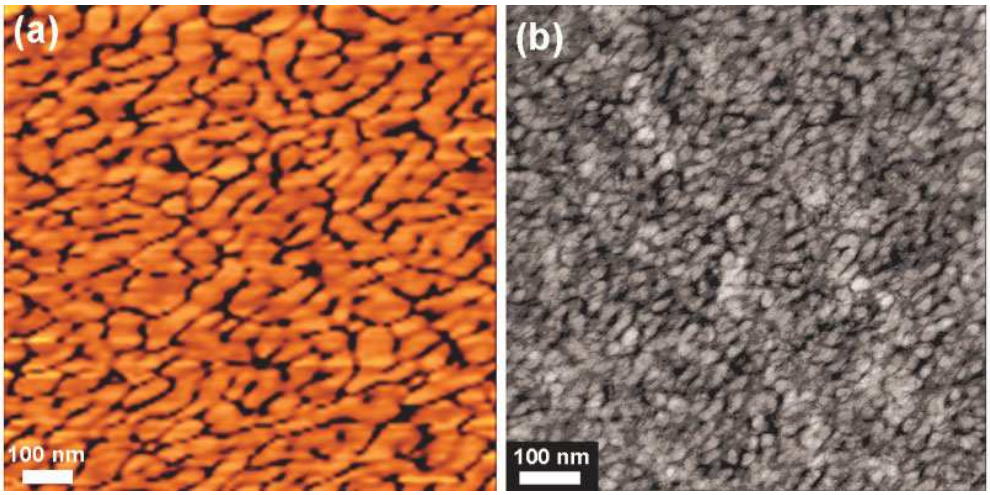

Figure 3. (a) AFM tapping phase image, and (b) TEM image for triblock copolymer membrane **3**(*X*70) with IEC of 1.28 meq./g.

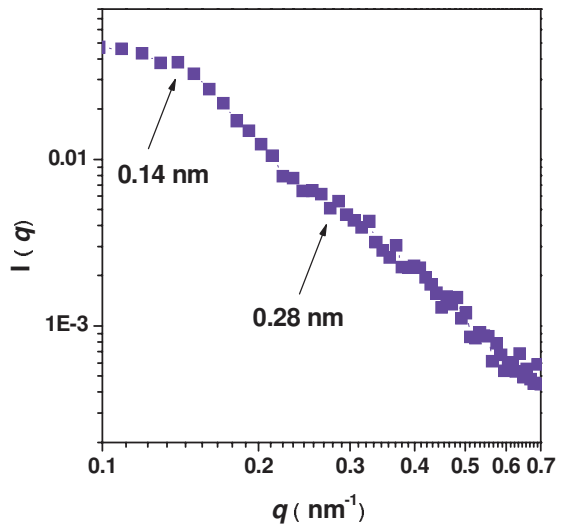

Figure 4. Small angle X-ray scattering (SAXS) of triblock copolymer **3**(*X*70) membrane.

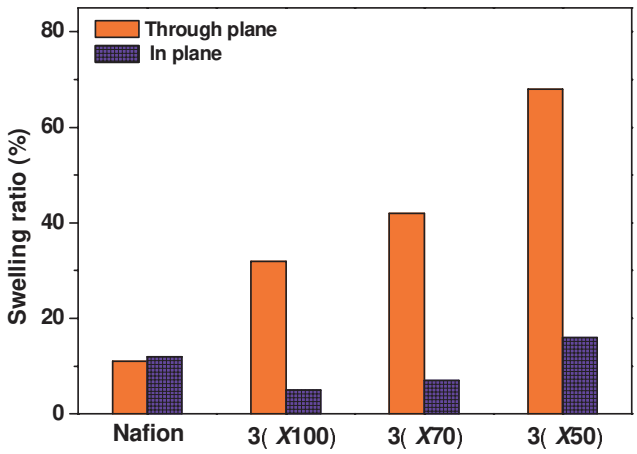

Figure 5. Comparison of dimensional swelling data for copolymers **3** and Nafion membranes at room temperature in water.

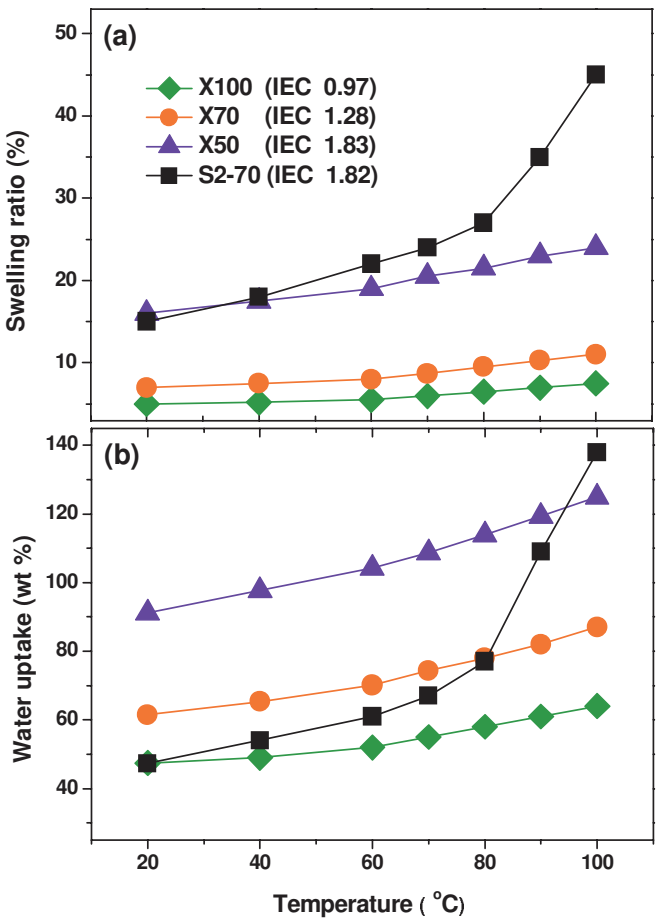

Figure 6. (a) The water uptake and (b) swelling ratio in-plane direction dependence of temperature in water. (The data of S2-70 from ref. [49])

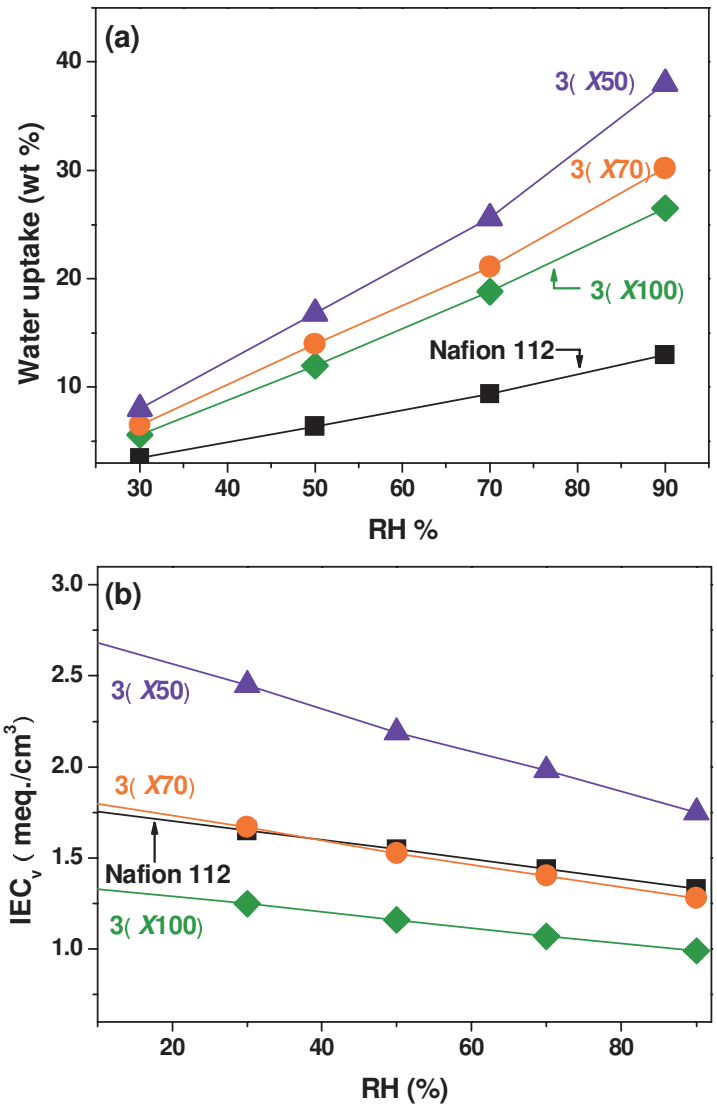

Figure 7. (a) Water uptake and (b) volumetric IEC_v for copolymer **3** membranes and Nafion 112 as a function of relative humidity at 90 ^oC.

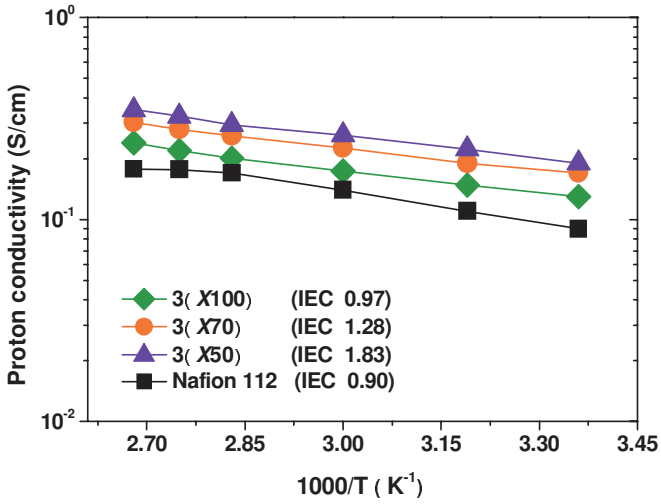

Figure 8. Proton conductivity of **3** membranes under fully hydrated state (in water) as a function of temperature.

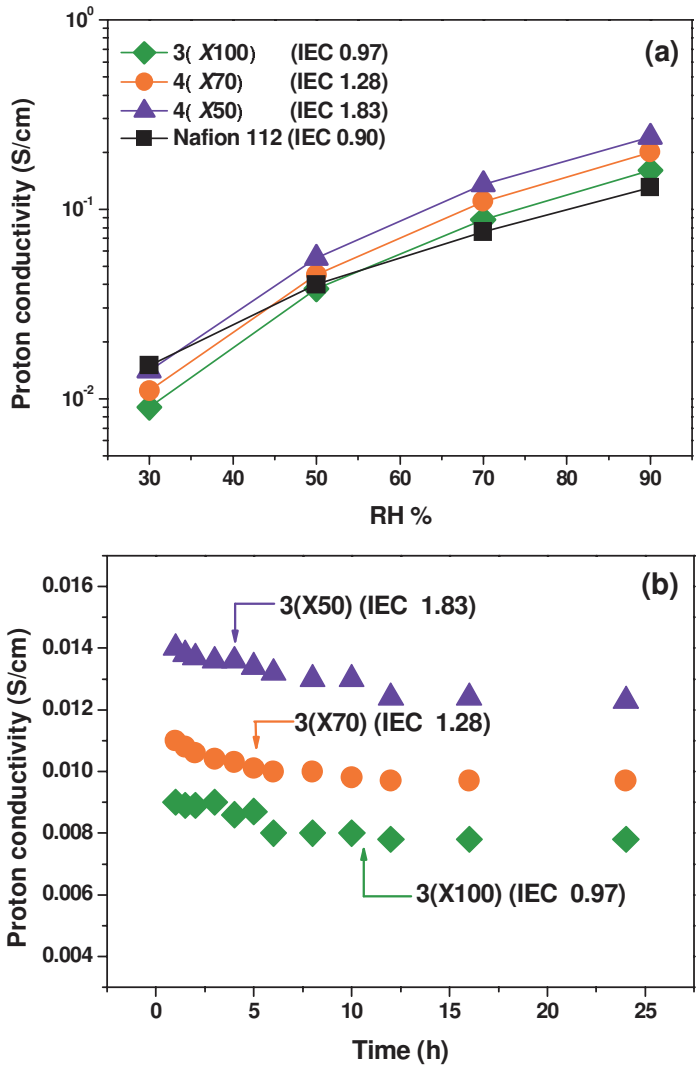

Figure 9. (a) Water uptake and proton conductivity of **3** membranes at 90 °C as a function of RH, (b) proton conductivity as a function of test time at 30 % RH and 90 °C.

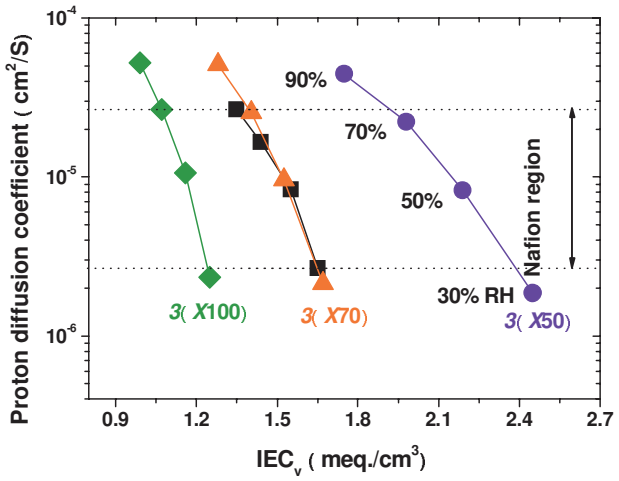

Figure 10. Proton diffusion coefficients of **3** and Nafion 112 membranes as a function of volumetric IEC_v at 90 °C.

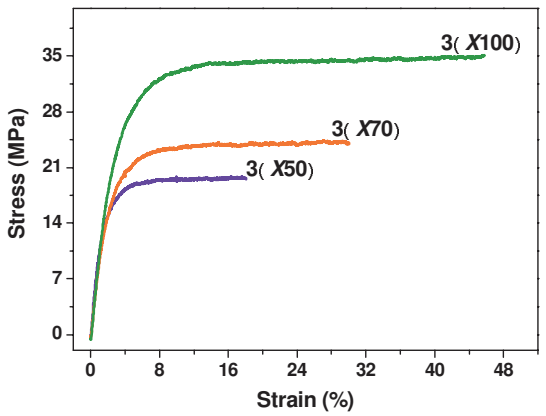

Figure 11. Stress *vs* strain curves of triblock copolymer **3** membranes at room temperature and 50 % RH.

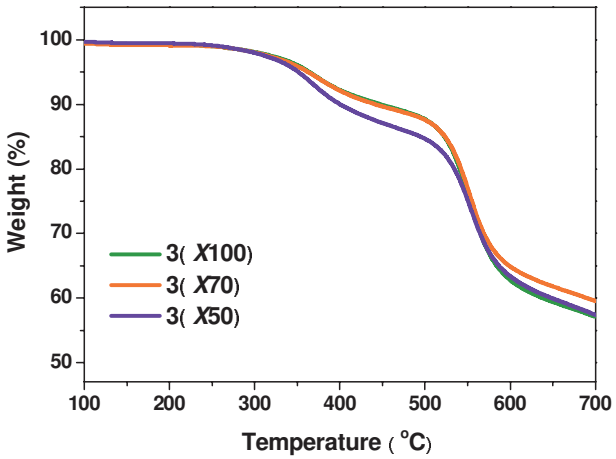

Figure 12. TGA curves for triblock copolymer **3** membranes from measurements run at 10 °C/min in N_2.

Table 1. Properties of the polymers **1**, **2** and **3**.

samples	1			2	3				
	M_n	M_w/M_n	$\eta^{a)}$ (g dL^{-1})	$\eta^{a)}$ (g dL^{-1})	$\eta^{b)}$ (g dL^{-1})	IEC (NMR) (meq./g)	IEC (titr.) (meq./g)	DS	T_g (°C)
*X*100	52000	1.6	0.48	0.57	1.12	0.91	0.97	100	203
*X*70	36000	1.4	0.41	0.47	1.04	1.33	1.28	100	209
*X*50	24000	1.7	0.36	0.38	0.91	1.86	1.83	100	213

[a)] 0.5 g dL^{-1} in NMP at 30 °C; [b)] 0.5 g dL^{-1} in DMSO at 30 °C.

Table 2. Various IEC, water uptake and proton conductivities of **3** and Nafion 112 membranes in water at 20 °C.

samples	density (g/cm^3)	IEC_w (meq./g)	IEC_v (meq./cm^3)		water uptake			conductivity	
			dry	wet	wt %	λ	vol %	mS/cm	D_σ (cm^2/S)
3(*X*100)	1.39	0.97	1.35	0.81	47.4	27.1	65.9	130	4.2×10^{-5}
3(*X*70)	1.43	1.28	1.83	0.97	61.5	26.7	87.9	170	4.6×10^{-5}
3(*X*50)	1.50	1.83	2.74	1.16	91.2	27.7	136.8	190	4.3×10^{-5}
Nafion 112	1.98	0.90	1.78	1.29	19.3	12.0	37.6	90	1.8×10^{-5}

Fully aromatic triblock copolymers as PEMs: highly proton conducting system based aryl-based triblock copolymers are developed. The unique polymer architecture brought about by nanophase separation between the extreme opposing hydrophobic and hydrophilic domains is responsible for the high proton diffusion coefficients, and thus high proton conductivities, throughout a wide range of relative humidity conditions.

Keyword: triblock copolymer; nanochannel; proton transport; fuel cell; polymer exchange membrane

Nanwen Li, So Young Lee, Ying-Ling Liu, Young Moo Lee *, Michael D. Guiver *

Highly proton-conducting fully aromatic triblock copoly(arylene ether sulfone)s